nature COMMUNICATIONS

ARTICLE

Received 10 Jun 2014 | Accepted 23 Nov 2014 | Published 12 Jan 2015

DOI: 10.1038/ncomms6929

Multi-body coalescence in Pickering emulsions

Tong Wu[1,*], Haitao Wang[1,*], Benxin Jing[2], Fang Liu[3], Peter C. Burns[1,4] & Chongzheng Na[1]

Particle-stabilized Pickering emulsions have shown unusual behaviours such as the formation of non-spherical droplets and the sudden halt of coalescence between individual droplets. Here we report another unusual behaviour of Pickering emulsions—the simultaneous coalescence of multiple droplets in a single event. Using latex particles, silica particles and carbon nanotubes as model stabilizers, we show that multi-body coalescence can occur in both water-in-oil and oil-in-water emulsions. The number of droplets involved in the *n*th coalscence event equals four times the corresponding number of the tetrahedral sequence in close packing. Furthermore, coalescence is promoted by repulsive latex and silica particles but inhibited by attractive carbon nanotubes. The revelation of multi-body coalescence is expected to help better understand Pickering emulsions in natural systems and improve their designs in engineering applications.

[1] Department of Civil and Environmental Engineering and Earth Sciences, University of Notre Dame, 156 Fitzpatrick Hall, Notre Dame, Indiana 46556, USA. [2] Department of Chemical and Biomolecular Engineering, University of Notre Dame, 182 Fitzpatrick Hall, Notre Dame, Indiana 46556, USA. [3] Department of Applied and Computational Mathematics and Statistics, University of Notre Dame, 153 Hurley Hall, Notre Dame, Indiana 46556, USA. [4] Department of Chemistry and Biochemistry, University of Notre Dame, 251 Nieuwland Science Hall, Notre Dame, Indiana 46556, USA. * These authors contributed equally to this work. Correspondence and requests for materials should be addressed to C.N. (email: chongzheng.na@gmail.com).

Pickering emulsions are made of particle-stabilized droplets suspended in an immiscible continuous liquid phase[1,2]. They are important soft matter systems that form naturally in crude oils[3] and food products[4] and have been engineered for drug delivery[5], water purification[6] and material processing[7–10]. Compared with ordinary emulsions, Pickering emulsions are distinctively stable because the removal of interfacial particles requires a large amount of energy[11]. When individual Pickering droplets are forced to coalesce, the extraordinary stability brought about by interfacial particles can lead to the formation of non-spherical droplets[12–14] and the arrest of droplet coalescence[15,16]. Little is known, however, about the coalescence of a collection of hundreds and thousands of Pickering droplets as in real emulsions. This is particularly important when particle stabilizers are used to produce near-monodispersed droplets[17], during which the distribution of droplet size can be significantly broadened by coalescence under gravity, floatation and shear[18,19].

Here we report for the first time that the presence of stabilizers at the oil–water interface can lead to multi-body coalescence in an ensemble of Pickering droplets—a phenomenon that has not been reported for either Pickering or ordinary emulsions. More interestingly, the number of droplets involved in coalescence equals four times the corresponding number of the tetrahedral sequence, indicating the inclusion of all closely packed nearest neighbours in a single coalescene event. As a result, a magic size distribition is produced with distinctive maxima related to each other through the cubic root of four times the tetrahedral numbers. Futhermore, interactions between stabilizers are found to affect the probability of coalescence by varying interfacial tension. Using model stabilizers including latex particles, silica particles and carbon nanotubes (CNTs), we show that coalescence is promoted by interparticle repulsion but inhibited by interparticle attraction.

Results

Selection of emulsion systems. To investigate coalescence of Pickering droplets in an ensemble, we select three representative emulsion systems, including latex particle-stabilized water droplets in dodecane, silica particle-stabilized 1,2-dichlorobenzene (DCB) droplets in water and CNT-stabilized water droplets in dodecane. Comparisons between the first two systems will show that multi-body coalescence occurs in both water-in-oil and oil-in-water emulsions. Subsequent comparisons with the CNT system will reveal differences between stabilizers lacking and having attractive interactions. Our results are organized in four sections as follows, including emulsion preparation and droplet size analysis, evolution of droplet size through multi-body coalescence, polydispersity and size evolution and coalescence probability and interparticle force.

Emulsion preparation and droplet size analysis. The three stabilizers and typical Pickering emulsions made from them are shown in Fig. 1. Latex and silica particles (Fig. 1a,b) are spheres with diameters of 0.8 μm and 1 μm, respectively. CNTs decorated

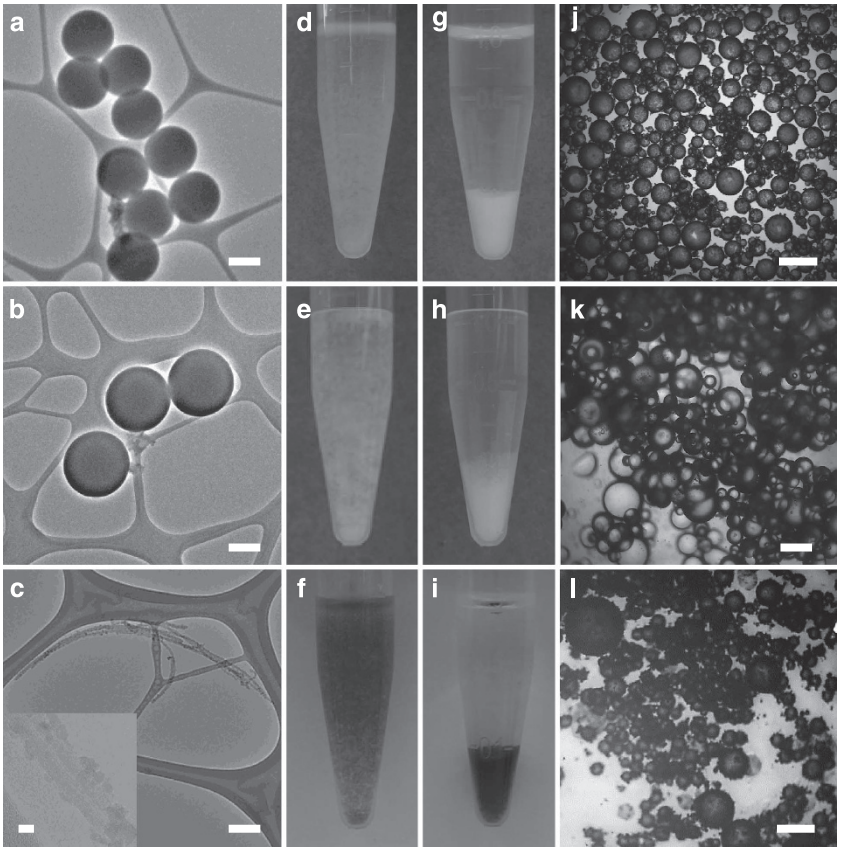

Figure 1 | Pickering emulsions made of three types of stabilizers. Results obtained with different analytical techniques are organized in columns: (**a**–**c**) transmission electron micrographs of stabilizers, (**d**–**f**) digital photographs of emulsions during mixing, (**g**–**i**) photographs taken at the end of standing and (**j**–**l**) optical micrographs of emulsions after standing. Results obtained with different stabilizers are organized in rows: (**a**,**d**,**g**,**j**) latex particle-stabilized water droplets in dodecane, (**b**,**e**,**h**,**k**) silica particle-stabilized 1,2-dichlorobenzene (DCB) droplets in water and (**c**,**f**,**i**,**l**) carbon nanotube-stabilized water droplets in dodecane. Mass ratio between droplets and the continuous phase: (**d**,**g**,**j**), 0.0667; (**e**,**h**,**k**), 0.0650; (**f**,**i**,**l**), 0.0667. Stabilizer-to-droplet mass ratio: (**d**,**g**,**j**), 0.02; (**e**,**h**,**k**), 0.03; (**f**,**i**,**l**), 0.02. Scale bars: **a**–**c**, 500 nm; inset in **c**, 5 nm and **j**–**l**, 250 μm.

with surface tension-tuning magnetite (Fe_3O_4) nanoparticles (Fig. 1c) are several micrometers long and have a diameter of ca. 15 nm (ref. 6). Pickering emulsions stabilized by latex particles, silica particles and CNTs are prepared following a conventional protocol[20], involving two consecutive steps. First, water, oil and stabilizers are mixed and then shaken vigorously by hand for 10 min (Fig. 1d–f), forming Pickering emulsions containing stabilizer-wrapped droplets[21]. Then, emulsions are left standing undisturbed on top of a bench for 10 min, allowing droplets to precipitate (Fig. 1g–i), forming a closely packed ensemble (Fig. 1j–l) to induce coalescence. Pickering droplets prepared following this protocol have low uniformity indices between 0.2 and 0.4 (Supplementary Fig. 1)[22–24], suggesting that the emulsions have only experienced limited coalescence[21].

After coalescence is complete, diameters of at least 500 droplets are measured using an optical microscope. Histograms, as shown in Fig. 2a–c, are constructed to facilitate detailed analyses of droplet size distribution. For all three types of emulsions, the diameter histogram can be readily deconvoluted into a series of Gaussian functions, indicating that each emulsion consists of several normally distributed populations of droplets. Of note, deconvolution is only possible when histograms are generated using at least 500 measurements. Similar histograms reported in the literature are usually made with significantly less measurements, often in the order of 50–100 (ref. 21). Under such conditions, the combination of multiple normal distributions degenerates to a single log-normal distribution[25].

The mean of each deconvoluted normal distribution, d_n ($n=0$, 1, 2, 3), represents the mean diameter of the corresponding droplet population. We find that d_n decreases with increasing stabilizer-to-droplet mass ratio α, as shown in Fig. 2d–f. The inverse dependence of d_n on α can be readily explained by matching the total surface area of droplets and the total cross-section area of interfacial stabilizers[25]:

$$d_n = 6\rho(1-\eta)\tau_n\alpha^{-1}, \quad (1)$$

where ρ is the specific gravity of stabilizers with respect to the droplet phase, η is the porosity of interfacial packing and τ_n is packing thickness. Conformation of experimental data to equation (1) indicates that fulfiling the interfacial area requirement for accommodating all stabilizer particles is an important determinant of droplet size.

We further compare d_n ($n>0$) with d_0, revealing a linear relationship between them:

$$d_n = k_n d_0;\ n = 1,\ 2,\ \text{or } 3, \quad (2)$$

as shown in Fig. 2g–i. The scaling factor k_n is estimated from the slope of linear regression. For $n=1$, 2 and 3, $k_1 \approx 1.6$, $k_2 \approx 2.5$ and

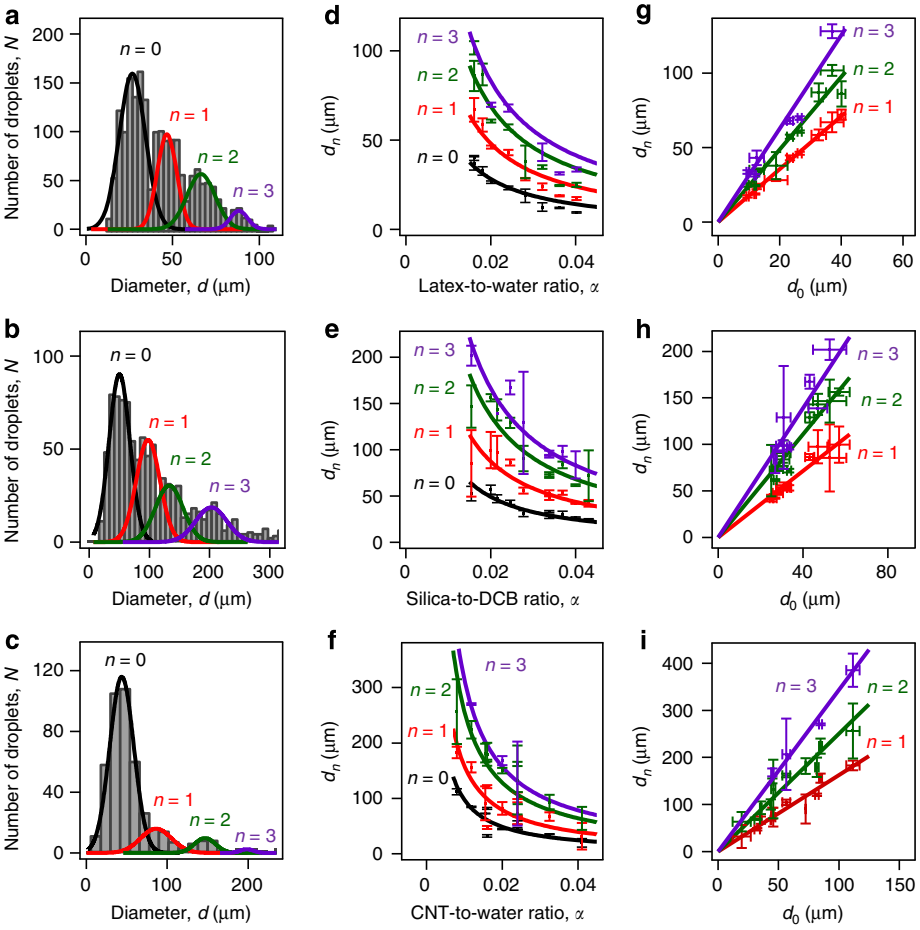

Figure 2 | Size distributions of three types of Pickering droplets. Results of different analyses are organized in columns: (**a**–**c**) diameter histograms showing distinctive maxima: d_n's ($n=0$, 1, 2, 3), (**d**–**f**) inverse correlations of d_n's with stabilizer-to-droplet mass ratio α and (**g**–**i**) linear correlations of d_n's ($n>0$) with d_0. Results for different stabilizers are organized in rows: (**a**,**d**,**g**) latex particle-stabilized water droplets in dodecane, (**b**,**e**,**h**) silica particle-stabilized 1,2-dichlorobenzene (DCB) droplets in water and (**c**,**f**,**i**) carbon nanotube-stabilized water droplets in dodecane. Curves in **d**–**f** are least-square regressions to equation (1). Lines in **g**–**i** are regressions to equation (2). Mass ratio between droplets and the continuous phase: (**a**,**d**,**g**), 0.0667; (**b**,**e**,**h**), 0.0650; (**c**,**f**,**i**), 0.0667. Stabilizer-to-droplet mass ratio: **a**, 0.02; **b**, 0.03 and **c**, 0.02. Error bars represent s.e.

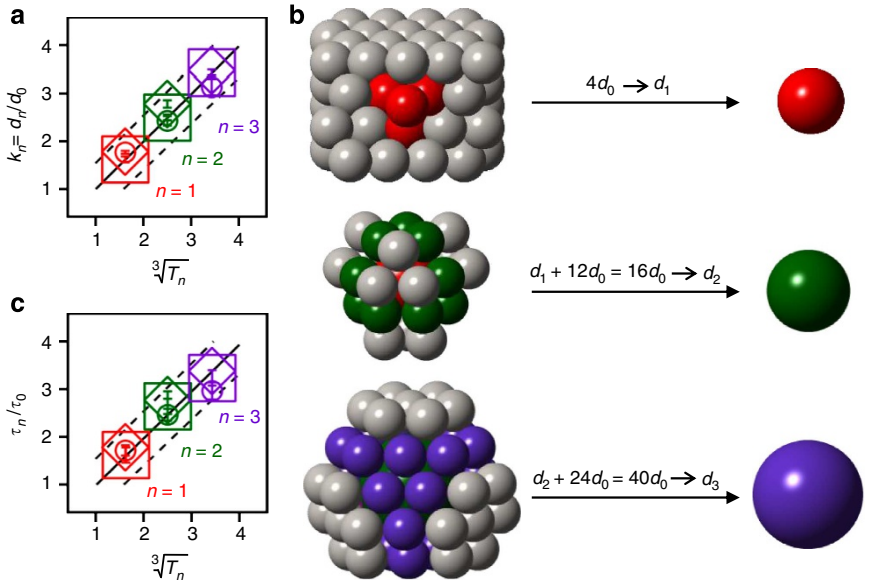

Figure 3 | Scaling of Pickering droplet diameters according to the tetrahedral number sequence. (**a**) Correlation of the scaling factor $k_n = d_n/d_0$ ($n = 1, 2, 3$) with the cubic root of four times the tetrahedral number, T_n. (**b**) Formation of d_n droplets from the coalescence of one d_{n-1} droplet (no d_{n-1} droplet for $n = 1$) and ($T_n - T_{n-1}$) d_0 droplets in face-centred close packing. Note: droplets coloured in grey do not participate in coalescence. (**c**) Increase of interfacial particle thickness after coalescence. Extra-large symbols in **a** and **c** are used for clarity of presentation: squares, latex particle-stabilized water droplets in dodecane; diamonds, silica particle-stabilized 1,2-dichlorobenzene droplets in water; circles, carbon nanotube-stabilized water droplets in dodecane. Solid lines in **a** and **c** are least-square regressions ($R^2 = 0.99$). Dashed lines are 95% confidence intervals. Error bars represent s.e.

Table 1 | Progression of coalescence in FCC packing*.

n	Nearest Neighbors†	Droplets Involved in the *n*th Coalescence	
		All Droplets Involved	Frontal Droplets Removed‡
1	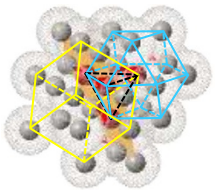		
2	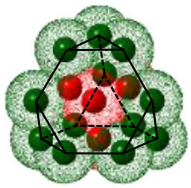	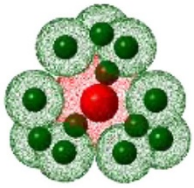	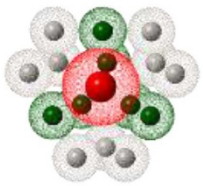
3	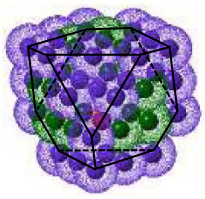	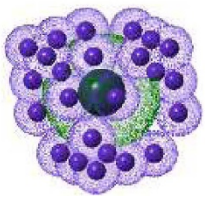	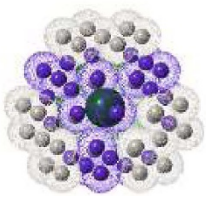

CNT, carbon nanotube; FCC, face-centred close.
*Thickness of the CNT layer is exaggerated for visual effects. Grey droplets are not nearest neighbours and do not participate in coalescence.
†The close-packed [111] plane is marked in orange. The FCC unit cell is marked by yellow lines. The tetradecahedron formed by 12 coordinating neighbours around a central d_0 droplet is marked by cyan lines. The octahedron (tetrahedron for $n = 1$) formed by coalescing droplets is marked by black lines.
‡To illustrate that only certain enclosing neighbours can coalesce with the droplet (an interstitial void for $n = 1$) in the centre.

$k_3 \approx 3.4$ for all three emulsion systems. The conservation of k_n's among different emulsion systems suggests the presence of a univeral mechanism that controls the evolution of droplet size.

Evolution of droplet size through multi-body coalescence. To elucidate the mechanism of size evolution for Pickering droplets, we first focus on the mean diameter of deconvoluted droplet

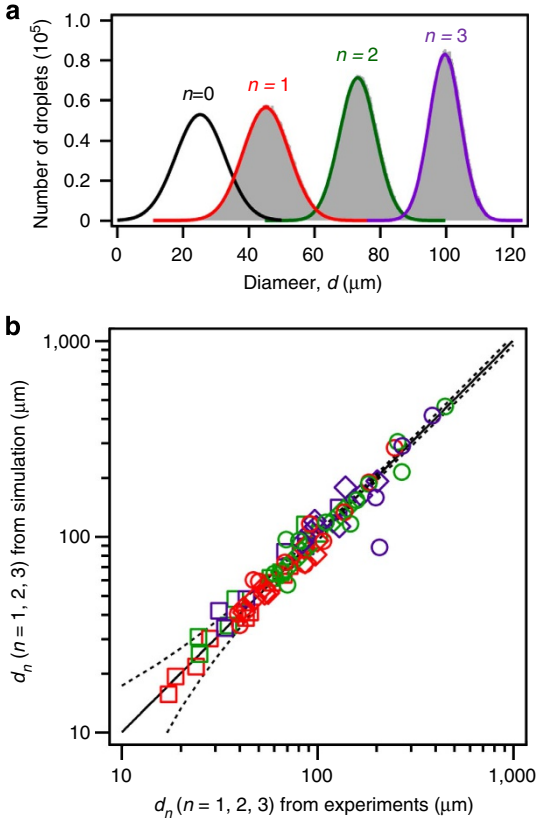

Figure 4 | Evolution of diameter distribution through coalescence examined by Monte Carlo simulation. (**a**) Evolution of the normal distribution of d_0 with a mean of 25.3 μm and a s.d. of 7.5 μm (zeroth population in Fig. 2a) through multi-body coalescence (grey shades, simulated populations; coloured curves, Gaussian fits). (**b**) Comparison of mean diameters of d_n's ($n=1$, 2, 3) obtained from fitting simulated data to Gaussian functions with those obtained from fitting experimental data to Gaussian functions. Symbols: squares, latex particle-stabilized water droplets in dodecane; diamonds, silica particle-stabilized 1,2-dichlorobenzene droplets in water; circles, carbon nanotube-stabilized water droplets in dodecane. Colours: red, $n=1$; green, $n=2$; purple, $n=3$. The solid line is obtained by linear regression ($R^2=0.96$). Dashed curves bracket 95% confidence intervals.

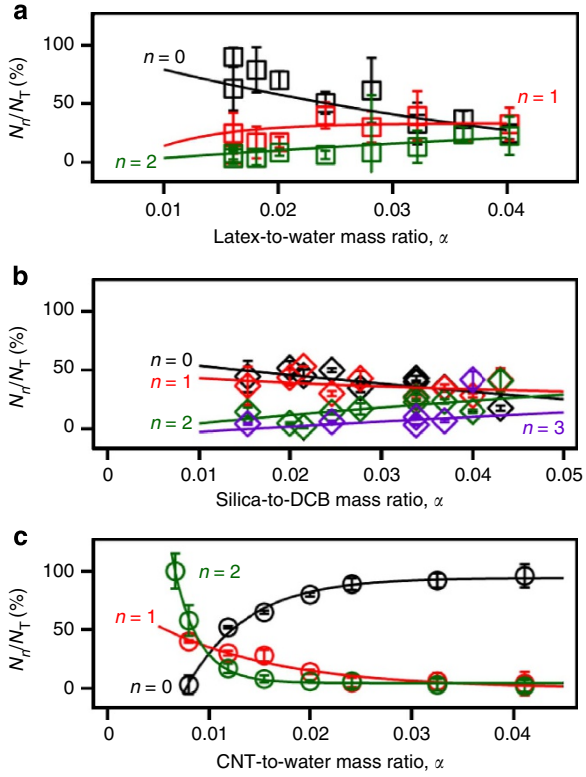

Figure 5 | Relative abundances of Pickering droplets from different normal populations. (**a**) Latex particle-stabilized water droplets in dodecane (**b**) Silica particle-stabilized 1,2-dichlorobenzene (DCB) droplets in water. (**c**) Carbon nanotube (CNT)-stabilized water droplets in dodecane. $N_T=\sum_{i=0}^{3}N_i$ is the total number of droplets from all populations. Curves are regressions to exponential functions ($R^2>0.8$). Error bars represent the standard deviation of the data.

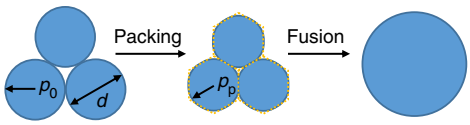

Figure 6 | Two consecutive processes of coalescence. Packing presses droplets together and transforms them from spheres to rounded polyhedrons. Fusion between droplets then occurs with the rupture of the separating liquid film to complete coalescence.

population without considering dispersion of the population. As shown in Fig. 3a (see Supplementary Table 1 for data), k_n equals the cubic root of four times the corresponding tetrahedral number, T_n:

$$k_n=\sqrt[3]{T_n};\ T_n=\sum_{j=1}^{n}2j(j+1), \qquad (3)$$

suggesting that a d_n droplet has the same volume as T_n d_0 droplets and thus is formed by their coalescence. For $n=1$, 2 and 3, $T_n=4$, 16 and 40; therefore, the coalescence of these Pickering droplets is multi-body in nature.

Multi-body coalescence requires droplets to be closely packed, which is facilitated by the density difference between water and oil in our experimental systems (*cf.* Fig. 1g–i)[26]. As illustrated in Fig. 3b and Table 1, four nearest-neighbouring d_0 droplets form a tetrahedron in a face-centred close (FCC) packed ensemble. When all four droplets coalesce simultaneously, the new droplet has a diameter of $d_1=\sqrt[3]{T_1}d_0$, where $T_1=4$. The d_1 droplet has 12 nearest d_0 neighbours in FCC, yielding a d_2 droplet after coalescing with the d_1 droplet: $d_2=\sqrt[3]{T_2}d_0$, where $T_2=4+12=16$. Similarly, a d_3 droplet is formed by the coalescence of the d_2 droplet with its 24 nearest neighbours: $d_3=\sqrt[3]{T_3}d_0$, where $T_3=16+24=40$.

We further examine multi-body coalescence by considering the material conservation of interfacial stabilizers before and after coalescence, which requires:

$$T_n\rho(1-\eta)\tau_0\pi d_0^2=\rho(1-\eta)\tau_n\pi d_n^2. \qquad (4)$$

By combining this equation with equation (2), we obtain:

$$\tau_n/\tau_0=\sqrt[3]{T_n}=k_n, \qquad (5)$$

for constants ρ and η. Indeed, equation (5) holds for all three emulsion systems as illustrated in Fig. 3c (see Supplementary Table 2 for data).

Polydispersity and size evolution. In the analyses described above, we have assumed that each deconvoluted droplet population has a single diameter, d_n ($n=0$, 1, 2, 3), equal to the mean

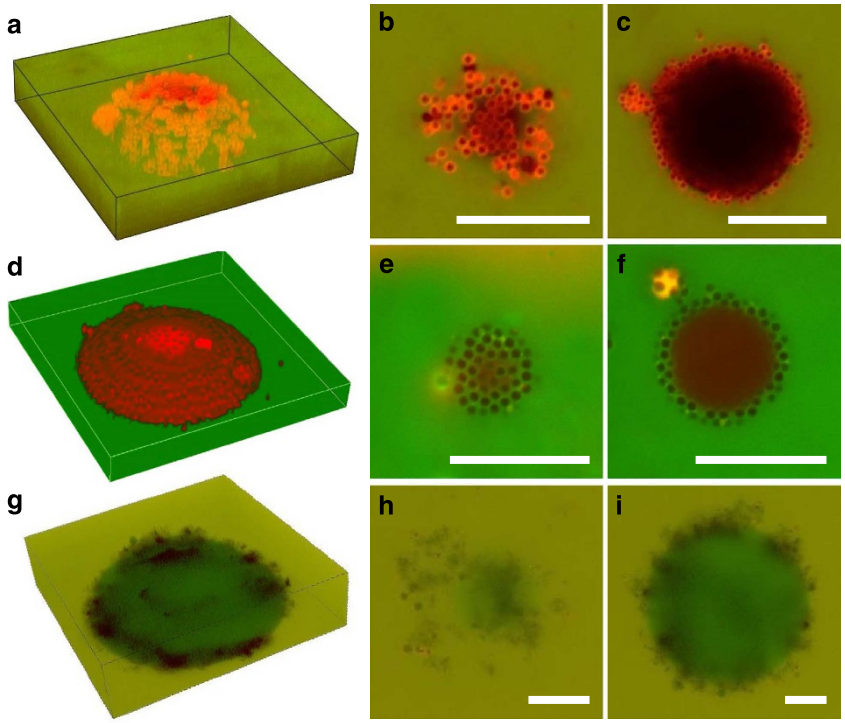

Figure 7 | False-colour confocal laser scanning micrographs of interfacial stabilizers. Images obtained with different stabilizers are organized in rows: (**a**–**c**) latex particle-stabilized water droplets in dodecane, (**d**–**f**) silica particle-stabilized 1,2-dichlorobenzene droplets in water and (**g**–**i**) carbon nanotube-stabilized water droplets in dodecane. Different types of images are organized in columns: (**a**,**d**,**g**) three-dimensional reconstructions of spherical caps, (**b**,**e**,**h**) cross-sections at the tops of spheres and (**c**,**f**,**i**) cross-sections below the tops. Note: the diameter of individual carbon nanotubes is much smaller than the imaging resolution (ca. 300 nm); therefore, individual nanotubes and bundles of a few nanotubes are not visually resolved. Mass ratio between droplets and the continuous phase: (**a**–**c**), 0.0667; (**d**–**f**), 0.0650 and (**g**–**i**), 0.0667. Stabilizer-to-droplet mass ratio: (**a**–**c**), 0.02; (**d**–**f**), 0.03 and (**g**–**i**), 0.01. Scale bars, 10 μm.

of the Gaussian fit of experimental data. For the 0th droplet population, this assumption can be validated by considering that d_0 droplets are formed under vigorous shaking—an independent and identical process with a finite variance[27]. However, will the coalescence of normally distributed d_0 droplets produce normally distributed d_n ($n>0$) droplets?

Coalescence progresses through the conservation of volume:

$$d_n^3 = \sum_{i=1}^{T_n} d_{0,i}^3. \qquad (6)$$

According to equation (6), we can prove that the probability density function of d_n is the T_n-fold convolution power of the probability density function of d_0^3 (see Supplementary Note 1 for derivation), which cannot be evaluated analytically. To obtain the distribution of the nth droplet population, we resort to the Monte Carlo method, which computes one million d_n values from randomly selected d_0's using equation (6).

The histograms of simulated d_n's ($n>0$) are shown in Fig. 4a, along with the normally distributed 0th population. The histograms can be well-approximated by normal distributions (similarity to normality >99.8%, as measured by Kolmogorov–Smirnov statistic)[28,29], confirming that the normal distribution is conserved through coalescence. The means of simulated d_n's are compared with those estimated from experimental data in Fig. 4b. The two data sets exhibit an excellent linear correlation with a near-unity slope of 1.01($\pm$0.01) ($R^2=0.96$), validating the use of Gaussian fits to estimate d_n's.

Coalescence probability and interparticle force. Although Pickering droplets prepared with different stabilizers coalesce following the same tetrahedral sequence, the selection of stabilizer can, however, affect coalescence probability. This is revealed by examining the variation of relative abundance N_n/N_T ($n=0, 1, 2, 3$) of each droplet population with α, as shown in Fig. 5. Here N_n is the number of d_n droplets estimated by integrating the nth Gaussian fit and $N_T=\sum_{i=0}^{3} N_i$. As α increases, N_n/N_T ($n>0$) increases at the expense of N_0/N_T for latex and silica-stabilized droplets (Fig. 5a,b), indicating that the addition of stabilizers promotes coalescence. For CNT-stabilized droplets (Fig. 5c), the opposite is observed, revealing improved stability of d_0 droplets and suppressed coalescence with the addition of CNTs.

To understand why coalescence is promoted by latex and silica particles but suppressed by CNTs, we divide coalescence into two consecutive processes: packing and fusion, as illustrated in Fig. 6. Packing presses d_0 droplets together and transforms them from spheres to rounded polyhedrons[30]. To pack droplets sufficiently close for coalescence, Laplace pressure p_0 must be overcome by the external pressure provided by the droplets' weight, P:

$$P>p_0; p_0=\frac{4\gamma}{d}, \qquad (7)$$

where γ is interfacial tension. Fusion between droplets then happens with the rupture of the separating liquid film, which requires the internal pressure of polyhedral droplets, p_p, to exceed the disjoining pressure of the film, Π (a property of the continuous phase)[31,32]:

$$p_p>\Pi; p_p=\frac{4\gamma}{d_0}C. \qquad (8)$$

where C is a constant related to droplet packing fraction.

Table 2 | Progression of coalescence in HCP*.

n	Nearest Neighbors†	Droplets Involved in the n^{th} Coalescence	
		All Droplets Involved	Frontal Droplets Removed‡
1	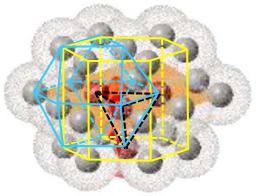		
2	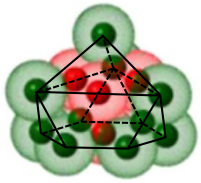	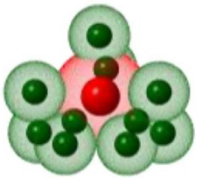	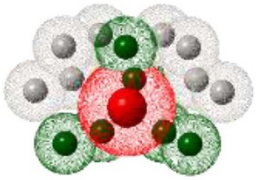
3	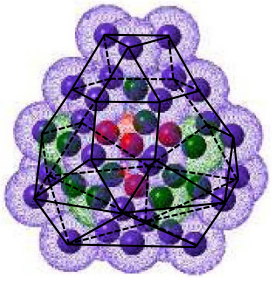	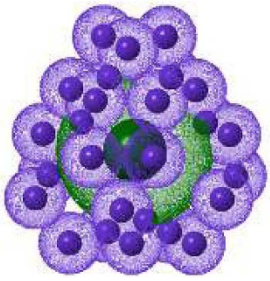	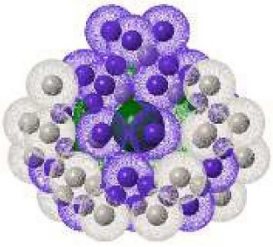

CNT, carbon nanotube; HCP, hexagonal close packing.
*Thickness of the CNT layer is exaggerated for visual effects. Grey droplets are not nearest neighbours and do not participate in coalescence.
†The close-packed [111] plane is marked in orange. The HCP unit cell is marked by yellow lines. The tetradecahedron formed by 12 coordinating neighbours around a central d_0 droplet is marked by cyan lines. The octahedron (tetrahedron for $n=1$) formed by coalescing droplets is marked by black lines.
‡To illustrate that only certain enclosing neighbours can coalesce with the droplet (an interstitial void for $n=1$) in the centre.

The interfacial tension includes contributions from both stabilizer-wrapped droplets, γ_d, and interactions between interfacial stabilizers, γ_s:

$$\gamma = \gamma_d + \gamma_s. \quad (9)$$

For stabilized droplets[2],

$$\gamma_d = \gamma_{ow}\left[1-(1-\eta)\cos^2\theta\right], \quad (10)$$

where γ_{ow} is the oil–water interfacial tension and θ is the contact angle formed by the continuous phase, the stabilizer surface and the droplet phase. According to equation (10), γ_d is constant for a given emulsion system; therefore, γ varies with γ_s.

γ_s can arise from the electrostatic repulsion between interfacial stabilizers. Latex particles, silica particles and CNTs are all negatively charged, as confirmed by their negative zeta potentials in water (latex, $-18(\pm 7)$ mV; silica, $-21(\pm 7)$ mV; CNTs, $-13(\pm 1)$ mV). Charge-induced repulsion, γ_{cp}, pushes stabilizer particles away from one another, reducing interfacial tension that pulls stabilizers together (that is, $\gamma_s = -\gamma_{cp} < 0$):

$$\gamma = \gamma_d - \gamma_{cp}. \quad (11)$$

An indication of interparticle repulsion is the random close packing[33] patterns formed by latex and silica particles at the oil–water interface and revealed by confocal laser scanning microscopy, as shown in Fig. 7a–c and d–f, respectively. With low γ, equation (7) is readily fulfiled. The probability of coalescence is thus controlled by the difference between p_p and Π according to equation (8). As α increases, d_0 decreases according to equation (1). This leads to an increase of p_p, improving the chances of overcoming Π to coalesce and produce more d_n ($n>0$) droplets at greater α (*cf.* Fig. 5a,b).

Different from latex and silica particles, CNTs form an extended network at the oil–water interface, as revealed by the confocal micrographs shown in Fig. 7g–i. Formation of the network can be attributed to strong π–π attractions between individual nanotubes, which overtake electrostatic repulsions between them (that is, $\gamma_s = \gamma_{\pi-\pi} - \gamma_{cp} > 0$)[6,34]:

$$\gamma = \gamma_d + \gamma_{\pi-\pi} - \gamma_{cp} \quad (12)$$

With high γ, equation (8) is readily fulfiled, leaving the control of coalescence probability to equation (7). As α increases, d_0 decreases and p_0 increases, resulting in a decrease of coalescence and minimal amounts of d_n ($n>0$) droplets with large α (*cf.* Fig. 5c).

Discussion

We have shown that closely packed Pickering droplets can coalesce through a multi-body mechanism. We hypothesize that the determining factor of multi-body coalescence is the presence of stabilizers at the oil–water interface, which slows down coalescence. In ordinary emulsions where droplets are stabilized by surfactant molecules or ions, coalescence happens rapidly between two droplets[35,36]. Recent measurements have, however, shown that coalescence between

two particle-stabilized droplets is orders of magnitude slower[37]. The extended transition time provides an opportunity for all of the nearest neighbours to be involved in a single coalescence event once coalescence is initiated between two droplets.

We formulate the multi-body coalescence theory in the FCC configuration. If Pickering droplets are packed in the hexagonal close packing (HCP) configuration, the number of droplets involved in the first coalescence event is the same as in FCC but decreases gradually for the second and third events, as illustrated in Table 2. The k_n values for HCP are 1.6, 2.4 and 2.5 compared with 1.6, 2.5 and 3.4 for FCC. According to experimentally determined k_n's, the packing of Pickering droplets is better represented by FCC. Nonetheless, multi-body coalescence requires only short-range ordering because significant coalescence occurs in the first few coordination shells surrounding an interstitial void. In the longer range, the lack of organization, such as that in random close packing[33], should not affect the outcome of multi-body coalescence in Pickering emulsions.

Methods

Reagents. Reagent-grade chemicals were purchased from Sigma-Aldrich and Fisher Scientific except where otherwise stated. Deionized (DI) water ($18.2\,M\Omega\,cm^{-1}$) used in solution making, washing and rinsing was generated using a Millipore system (Billerica, MA, USA) on site. We prepared Pickering emulsions by shaking and standing (see below)[20].

Latex particle-stabilized water droplets in dodecane. Latex particles were obtained by drying an aqueous solution in vacuum overnight. The particles were then dispersed in dodecane (99%, TCI America) at various concentrations. To make Pickering emulsions, 50 µl DI water was added to 1 ml dodecane. The mixture was shaken by hand vigorously for 10 min and then left standing on bench for 10 min.

Silica particle-stabilized DCB droplets in water. Silica particles were first coated with (3-aminopropyl)trimethoxysilane (APTMS, 97%) to modify their surface wettability[38]. To do so, 0.1 ml particle solution (10 wt%) was dried in an oven at 120 °C overnight and was then mixed with 10 ml toluene (≥99.8%) and 100 µl APTMS. The mixture was shaken for 2 h. The particles were washed with toluene five times and with ethanol three times. The particles were then dried in an oven overnight to remove residual ethanol and immersed in water before use. To make a Pickering emulsion, 50 µl 1,2-DCB (99%, Alfa Aesar) was added to 1 ml DI water with different concentrations of silica particles. The mixture was shaken by hand vigorously and left standing undisturbed following the same procedure for making latex-stabilized emulsions.

CNT-stabilized water droplets in dodecane. Magnetite-decorated CNTs were prepared using multi-walled CNTs synthesized by chemical vapour deposition[6]. Catalysts were removed by washing with nitric acid. CNTs were then decorated with 10-nm magnetite nanoparticles using the polyol reduction method[39]. To make a CNT-stabilized Pickering emulsion, CNTs were dispersed in 10 ml water by sonication for 10 min, followed by an addition of 0.5 ml dodecane. The mixture was shaken and left standing quiescently following the same protocol for making latex and silica-stabilized emulsions.

Optical microscopy. Diameters of particle-stabilized droplets were measured using images taken by an optical microscope (Motic BA300POL). To do so, emulsions were poured on either glass (for silica-stabilized droplets) or plastic (for latex and CNT-stabilized droplets) Petri dishes. The emulsions were then diluted with the corresponding continuous phases to minimize droplet overlapping in the imaging field. For each sample, ~30 images were taken randomly with a ×10 objective lens (resolution: 1.25 µm per pixel). Diameters were measured using software ImageJ[40]. A few droplets stabilized by silica particles (<5%) were found at the arrested coalescence state with non-spherical shapes (Supplementary Fig. 2). They were excluded in subsequent diameter analyses.

Confocal laser scanning microscopy. Interfacial stabilizers were visualized using a confocal laser scanning microscope (Nikon A1R) equipped with a ×100 Plan Apo total internal reflection fluorescence objective lens. The oil phases were illuminated using oil-soluble Nile red. Water was illuminated using Alex Fluor 488. Concentrations of the fluorescent dyes were: latex particle-stabilized water droplets in dodecane, 0.001 mM Alex Fluor 488 in water and 0.1 mM Nile red in dodecane; silica particle-stabilized DCB droplets in water, 0.03 mM Nile red in DCB and 0.01 mM Alex Fluor 488 in water; CNT-stabilized water droplets in dodecane, 0.01 mM Alex Fluor 488 in water and 0.03 mM Nile red in dodecane. The oil-in-water emulsion stabilized by silica particles was imaged using a custom-made hydrophilic glass reservoir. To image water-in-oil emulsions stabilized by latex particles and CNTs, the reservoir was treated with a 1:100 octadecyltrichlorosilane toluene solution to create a hydrophobic coating before use.

Measurement of particle surface charge. Zeta potentials of latex particles, silica particles and CNTs were measured using a ZetaPlus analyzer (Brookhaven Instruments) in water at concentrations of $0.2\,mg\,l^{-1}$, $0.2\,mg\,l^{-1}$ and $0.12\,mg\,l^{-1}$, respectively. Water pH was adjusted according to the conditions in corresponding emulsions. Latex particles and CNTs were dispersed in water in equilibrium with atmospheric carbon dioxide at pH 5.6. Silica particles were dispersed in dilute sodium hydroxide solution at pH 7.0. Before measurements, stabilizer suspensions were sonicated for 30 min. For each stabilizer, five measurements were made.

References

1. Pickering, S. U. Emulsions. *J. Chem. Soc.* **91,** 2001–2021 (1907).
2. Binks, B. P. Particles as surfactants-Similarities and differences. *Curr. Opin. Colloid Interface Sci.* **7,** 21–41 (2002).
3. McLean, J. D. & Kilpatrick, P. K. Effects of asphaltene solvency on stability of water-in-crude-oil emulsions. *J. Colloid Interface Sci.* **189,** 242–253 (1997).
4. Dickinson, E. Food emulsions and foams: stabilization by particles. *Curr. Opin. Colloid Interface Sci.* **15,** 40–49 (2010).
5. Dinsmore, A. D. *et al.* Colloidosomes: selectively permeable capsules composed of colloidal particles. *Science* **298,** 1006–1009 (2002).
6. Wang, H. *et al.* Removal of oil droplets from contaminated water using magnetic carbon nanotubes. *Water Res.* **47,** 4198–4205 (2013).
7. Koos, E. & Willenbacher, N. Capillary forces in suspension rheology. *Science* **331,** 897–900 (2011).
8. Stratford, K., Adhikari, R., Pagonabarraga, I., Desplat, J. C. & Cates, M. E. Colloidal jamming at interfaces: a route to fluid-bicontinuous gels. *Science* **309,** 2198–2201 (2005).
9. Crossley, S., Faria, J., Shen, M. & Resasco, D. E. Solid nanoparticles that catalyze biofuel upgrade reactions at the water/oil interface. *Science* **327,** 68–72 (2010).
10. Velev, O. D., Lenhoff, A. M. & Kaler, E. W. A class of microstructured particles through colloidal crystallization. *Science* **287,** 2240–2243 (2000).
11. Aussillous, P. & Quere, D. Liquid marbles. *Nature* **411,** 924–927 (2001).
12. Subramaniam, A. B., Abkarian, M., Mahadevan, L. & Stone, H. A. Non-spherical bubbles. *Nature* **438,** 930–930 (2005).
13. Cui, M., Emrick, T. & Russell, T. P. Stabilizing liquid drops in nonequilibrium shapes by the interfacial jamming of nanoparticles. *Science* **342,** 460–463 (2013).
14. Abkarian, M. *et al.* Dissolution arest and stability of particle-covered bubbles. *Phys. Rev. Lett.* **99,** 188301 (2007).
15. Pawar, A. B., Caggioni, M., Ergun, R., Hartel, R. W. & Spicer, P. T. Arrested coalescence in Pickering emulsions. *Soft Matter* **7,** 7710–7716 (2011).
16. Whitby, C. P. & Krebsz, M. Coalescence in concentrated Pickering emulsions under shear. *Soft Matter* **10,** 4848–4854 (2014).
17. Nie, Z., Park, J. I., Li, W., Bon, S. A. F. & Kumacheva, E. An "inside-out" microfluidic approach to monodisperse emulsions stabilized by solid particles. *J. Am. Chem. Soc.* **130,** 16508–16509 (2008).
18. Hasmy, A., Paredes, R., Sonneville-Aubrun, O., Cabane, B. & Botet, R. Dynamical transition in a model for dry foams. *Phys. Rev. Lett.* **82,** 3368–3371 (1999).
19. Whitby, C. P., Fischer, F. E., Fornasiero, D. & Ralston, J. Shear-induced coalescence of oil-in-water Pickering emulsions. *J. Colloid Interface Sci.* **361,** 170–177 (2011).
20. Wiley, R. M. Limited coalescence of oil droplets in coarse oil-in-water emulsions. *J. Colloid Sci.* **9,** 427–437 (1954).
21. Arditty, S., Whitby, C. P., Binks, B. P., Schmitt, V. & Leal-Calderon, F. Some general features of limited coalescence in solid-stabilized emulsions. *Eur. Phys. J. E Soft Matter* **11,** 273–281 (2003).
22. Binks, B. P. & Whitby, C. P. Silica particle-stabilized emulsions of silicone oil and water: aspects of emulsification. *Langmuir* **20,** 1130–1137 (2004).
23. Romero, A., Cordobes, F., Puppo, M. C., Guerreroa, A. & Bengoechea, C. Rheology and droplet size distribution of emulsions stabilized by crayfish flour. *Food Hydrocolloids* **22,** 1033–1043 (2008).
24. Schmitt, V., Cattelet, C. & Leal-Calderon, F. Coarsening of alkane-in-water emulsions stabilized by nonionic poly(oxyethylene) surfactants: The role of molecular permeation and coalescence. *Langmuir* **20,** 46–52 (2004).
25. Wang, H. & Hobbie, E. K. Amphiphobic carbon nanotubes as macroemulsion surfactants. *Langmuir* **19,** 3091–3093 (2003).
26. Whitby, C. P., Lotte, L. & Lang, C. Structure of concentrated oil-in-water Pickering emulsions. *Soft Matter* **8,** 3784–3789 (2012).
27. Irani, R. R. *Particle Size: Measurement, Interpretation, and Application* (John Wiley & Sons, 1963).
28. Kolmogorov, A. N. Sulla determinazione empirica di una legge di distribuzione. *G. Ist. Ital. Attuari* **4,** 83–91 (1933).

29. Smirnov, N. Table for estimating the goodness of fit of empirical distributions. *Ann. Math. Stat.* **19,** 279–281 (1948).
30. Bibette, J., Morse, D. C., Witten, T. A. & Weitz, D. A. Stability criteria for emulsions. *Phys. Rev. Lett.* **69,** 2439–2442 (1992).
31. Princen, H. M. Highly concentrated emulsions I. cylindrical systems. *J. Colloid Interface Sci.* **71,** 55–66 (1979).
32. Princen, H. M., Aronson, M. P. & Moser, J. C. Highly concentrated emulsions II. Real systems. The effect of film thickness and contact angle on the volume fraction in creamed emulsions. *J. Colloid Interface Sci.* **75,** 246–270 (1980).
33. Clusel, M., Corwin, E. I., Siemens, A. O. N. & Brujic, J. A. 'Granocentric' model for random packing of jammed emulsions. *Nature* **460,** 611–615 (2009).
34. Feng, T., Hoagland, D. A. & Russell, T. P. Assembly of acid-functionalized single-walled carbon nanotubes at oil/water interfaces. *Langmuir* **30,** 1072–1079 (2014).
35. von Smoluchowski, M. Experiments on a mathematical theory of kinetic coagulation of coloid solutions. *Z. Phys. Chem. Stoechiom. Verwandtschafts.* **92,** 129–168 (1917).
36. Aldous, D. J. Deterministic and stochastic models for coalescence (aggregation and coagulation): a review of the mean-field theory for probabilists. *Bernoulli* **5,** 3–48 (1999).
37. Chen, G. *et al.* Coalescence of Pickering emulsion droplets induced by an electric field. *Phys. Rev. Lett.* **110,** 064502 (2013).
38. Krysztafkiewicz, A., Binkowski, S. & Wysocka, W. Pigments on amorphous silica carriers. *Powder Technol.* **132,** 190–195 (2003).
39. Wang, H., Cao, L., Yan, S., Huang, N. & Xiao, Z. An efficient method for decoration of the multiwalled carbon nanotubes with nearly monodispersed magnetite nanoparticles. *Mater. Sci. Eng. B* **164,** 191–194 (2009).
40. Schneider, C. A., Rasband, W. S. & Eliceiri, K. W. NIH Image to ImageJ: 25 years of image analysis. *Nat. Methods* **9,** 671–675 (2012).

Acknowledgements

C.N. thanks the Department of Energy Office of Nuclear Energy's Nuclear Energy University Programmes, the National Science Foundation Environmental Engineering Programme and the Notre Dame Sustainable Energy Initiative for financial support. P.C.B.'s contribution was supported by the Energy Frontier Research Center Materials Science of Actinides. We thank Kun-Yi Lin for performing preliminary experiments on carbon nanotubes. We thank Antonio Simonetti, Diogo Bolster and Kapil Khandelwal for their inspiring comments and suggestions.

Author contributions

C.N., H.W. and T.W. designed the study and analyzed data. T.W. and H.W. performed the experiments. B.J. contributed to the design of confocal measurements. F.L. performed Monte Carlo simulation and contributed to the statistical analysis of experimental data. P.C.B. contributed to the interpretation of droplet packing. All authors contributed to the writing of the paper.

Additional information

Supplementary Information accompanies this paper at http://www.nature.com/naturecommunications

Competing financial interests: The authors declare no competing financial interests.

Reprints and permission information is available online at http://npg.nature.com/reprintsandpermissions/

How to cite this article: Wu, T. *et al.* Multi-body coalescence in Pickering emulsions. *Nat. Commun.* 6:5929 doi: 10.1038/ncomms6929 (2015).